Investigating the Spatial Distribution of Integrin β_1 in Patterned Human Mesenchymal Stem Cells Using Super-Resolution Imaging

Ajay Tijore,[†] Srivats Hariharan,[§] Haiyang Yu,[†] Chee Ren Ivan Lam,[†] Feng Wen,[†] Chor Yong Tay,[‡] Sohail Ahmed,[§] and Lay Poh Tan*,[†]

[†]Division of Materials Technology, School of Materials Science and Engineering, Nanyang Technological University, 50 Nanyang Avenue, 639798, Singapore

[‡]Department of Chemical and Biomolecular Engineering, National University of Singapore, 4 Engineering Drive 4, 117585, Singapore

[§]Institute of Medical Biology, Agency for Science, Technology and Research (A*STAR), 8A Biomedical Grove, #06-06 Immunos, 138648, Singapore

S *Supporting Information*

ABSTRACT: Lineage commitment of human mesenchymal stem cells (hMSCs) could be directed through micro/nanopatterning of the extracellular matrix (ECM) between cells and substrate. Integrin receptors, integrator of the ECM and cell cytoskeleton, function as molecular bridges linking cells to different biophysical cues translated from patterned ECM. Here we report the distinct recruitment of active integrin β_1 (ITG-β_1) in hMSCs when they were committed toward the cardiomyogenic lineage on a micropatterned surface. In addition, a systematic study of the distribution of ITG-β_1 was performed on focal adhesions (FAs) using a direct stochastic optical reconstruction microscopy (dSTORM) technique, a super-resolution imaging technique to establish the relationship between types of integrin expression and its distribution pattern that are associated with cardiomyogenic differentiation of hMSCs. We ascertained that elongated FAs of ITG-β_1 expressed in patterned hMSCs were more prominent than FAs expressed in unpatterned hMSCs. However, there was no significant difference observed between the widths of FAs from both experimental groups. It was found in patterned hMSCs that the direction of FA elongation coincides with cell orientation. This phenomenon was however not observed in unpatterned hMSCs. These results showed that the biophysical induction methods like FAs patterning could selectively induce hMSCs lineage commitment via integrin-material interaction.

KEYWORDS: *hMSCs, integrin β_1, focal adhesion, cardiomyogenic differentiation, super-resolution imaging*
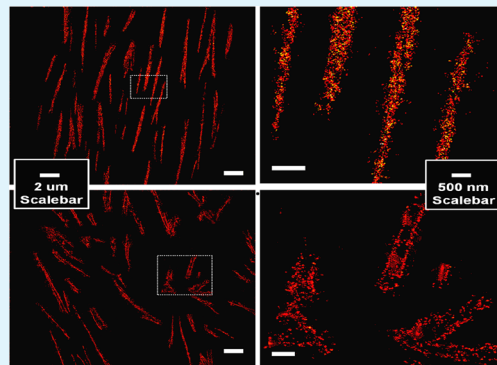
INTRODUCTION

Human mesenchymal stem cells (hMSCs) have gained popularity in the field of tissue engineering due to their ability to differentiate into specific cell types, vascular progenitor property and hypoimmunogenicity.[1,2] These features make hMSCs a potential candidate for stem cell based regenerative therapies. Targeted lineage-specific differentiation and the surrounding microenvironment are two of several other factors that play a key role in the accomplishment of such therapies. Among the aforementioned factors, the microenvironment, often described as the "stem cell niche", was shown to play a pivotal role to guide stem cell differentiation.[3-5] Biological and chemical induction methods for stem cell differentiation, though classical, have shortcomings such as uncontrolled cell growth, tumor formation, and cell death.[6] On the other hand, directed stem cell lineage commitment via biophysical means could potentially avoid these side effects. The patterning technique, a type of biophysical induction method, has been extensively used to investigate the stem cell behavior by controlling the extracellular matrix (ECM) localization.[7-9] The

ECM is an essential cell secreted component of the microenvironment of which cells finally adhere to.[6,10] Cellular interaction with the underlying matrix substratum is mediated via the transmembrane integrin receptors.[11-13] Such cell-matrix interaction triggers intracellular signaling cascades that recruit various adaptor proteins like vinculin, paxillin, etc. along with enzymes, linking actin cytoskeleton to ECM.[13-15] These ECM proteins, integrins, and cytoskeletal proteins assemble into aggregates and are known as focal adhesions collectively.[10,16] Focal adhesions are cell anchorage points at which intracellularly generated contractile forces are exerted onto the substrate.[17]

The roles of integrin in different cellular phenomenon like cell adhesion, proliferation, and differentiation have been comprehensively established.[10,14] Damsky et al. observed that surface expression of integrin β_1 changes when myoblasts fused
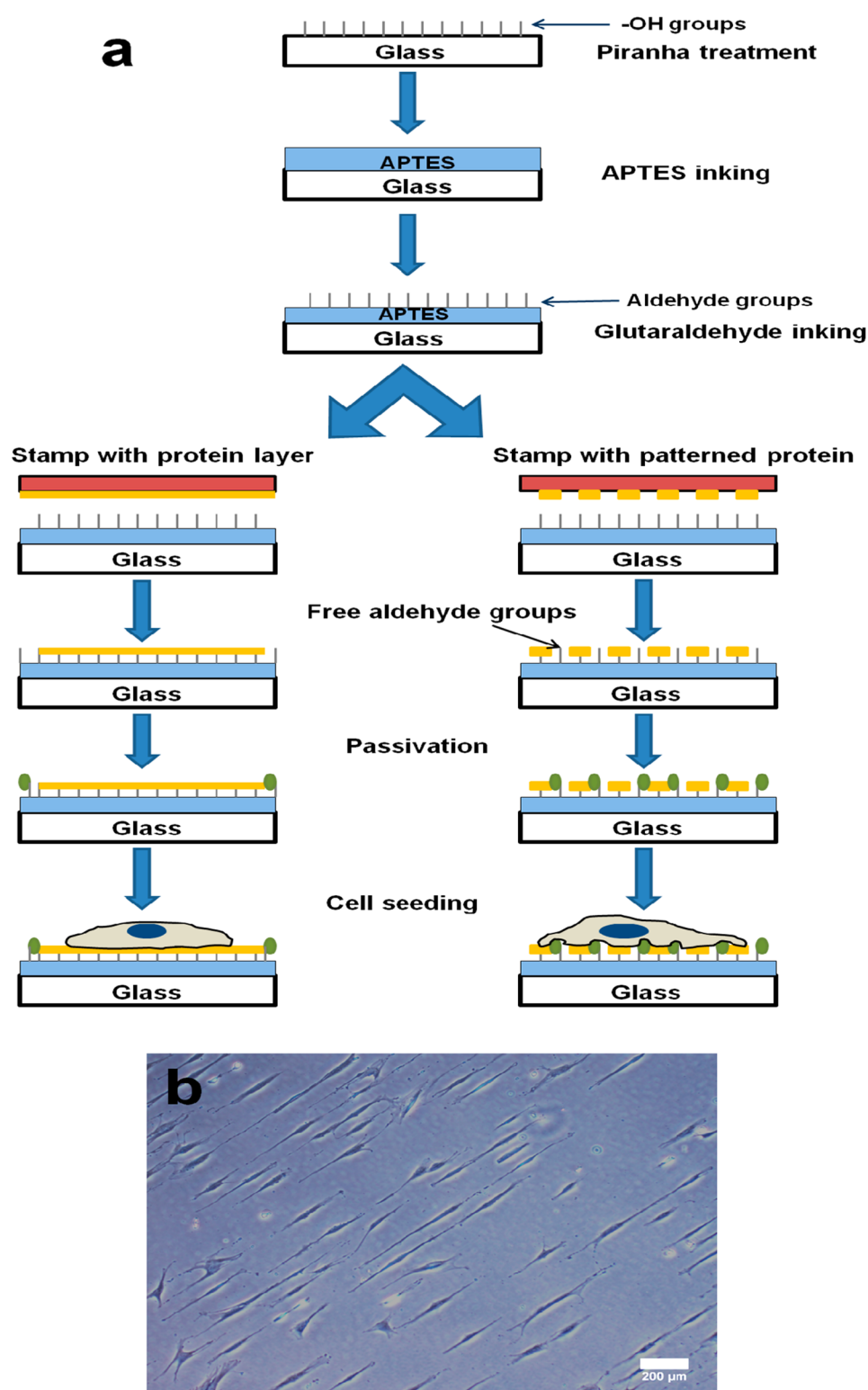
Figure 1. (a) Schematic illustration of the micropatterning procedure. The glass surface was treated with APTES and glutaraldehyde followed by inking with fibronectin. (b) Patterned hMSCs grown on the fibronectin micropattern printed glass substrate were captured 3 days after cell seeding. The scale bar is 200 μm.

to form myotubes.[18] Fassler et al. demonstrated the importance of integrin β_1 for cardiac muscle cell differentiation and specialization.[19] Adam et al. found that integrin $\alpha_5\beta_1$ was responsible for keratinocyte adhesion to fibronectin during terminal differentiation of the skin.[20] Yim et al. noticed that nanotopography influences hMSCs behavior by changing integrin clustering and focal adhesion assembly and in turn influences cell differentiation.[21] Altogether, these findings showed that cellular differentiation may be modulated via engineering integrin-substratum interactions.[22]

Directing stem cells fate through ECM micropatterning on cell substrate was well adapted in stem cell studies.[7,9,23] However, a detailed systematic study of cell-ECM interaction at the integrin receptor level has not been well documented yet. This is in part due to the diffraction limit of conventional fluorescence microscopy that does not allow one to visualize subcellular structures with a size of a few tens of nanometers and to provide insight into cellular structures. Recently, several super-resolution imaging methods that rely on precise position localization of single fluorophores have emerged. These methods include stimulated emission depletion (STED),[24] interferometric photoactivated localization microscopy (iPALM),[25] single particle tracking-PALM (sptPALM),[26] and direct stochastic optical reconstruction microscopy (dSTORM).[27] Stochastic photoswitching of fluorophores offers temporal separation of fluorophore emission which ultimately paved the path for one to visualize the molecular level structures with spatial resolution well beyond the diffraction limit. For example, researchers used three-dimensional super-resolution microscopy, an interferometric photoactivated localization microscopy to map the nanoscale organization of adaptor proteins in focal adhesions.[25] Recently, Rossier et al. published a study in which single particle tracking photo-activated localization microscopy was used to explore the dynamic nanoscale organization of integrin β_1 and β_3 inside the focal adhesions.[26]

In our previous work, we demonstrated a positive correlation between elongated hMSCs induced by micropatterning and cardiomyogenic commitment.[7,9,23,28] Further studies showed that focal adhesions of myocardial lineage committed hMSCs displayed distinct patterns as well.[8,29] As we attempt to move into nanolevel characterization of the integrins, conventional imaging systems could not reveal additional information like nanoscale distribution of integrins in focal adhesions (FAs). In this study, super-resolution imaging was used to capture the evolvement of integrins in hMSCs. It was hypothesized that integrin distribution pattern will differ significantly as the micropatterned cells are driven to commit myocardial lineage. This information would be essential for further elucidation of cell-material interactions and mechanotransduction events that follow. Here, we explore the distribution pattern of activated forms integrin β_1 (ITG-β_1) using the dSTORM technique in myocardial lineage committed hMSCs. Active ITG-β_1 is chosen as it was shown to be expressed significantly in hMSCs that commit to cardiomyogenesis (Figure S1, Supporting Information), and the ITG-β_1 blocking study using active ITG-β_1 antibodies confirmed the role of ITG-β_1 in myocardial differentiation of hMSCs (Figure S2, Supporting Information). Additionally, in several previous studies, the crucial role of ITG-β_1 during cardiomyogenesis has been highlighted. Fassler et al. demonstrated the lack of functions in cardiomyocytes differentiated from integrin β_1-deficient embryonic stem cells.[19] Further, Hescheler et al. observed that the regulation of voltage-dependent calcium channels via muscarinic (M2) receptor was absent in integrin β_1 knock out embryonic stem cell-derived cardiomyocytes.[30] In another study, Maitra et al. noticed that integrin β_1 could be responsible for cell attachment during cardiomyocyte cell cycle progression.[31]

■ EXPERIMENTAL SECTION

Fabrication of Patterned Elastomeric Stamp and Inking. Polydimethylsiloxane (PDMS) elastomeric stamps were used to ink the human plasma derived fibronectin (BD, Biosciences) onto glutaraldehyde (Sigma) treated Lab Tek two well chambered cover glasses (Nunc). The silicon master templates bearing desired topographic features were fabricated by standard photolithography[7] and were pretreated with 1% octadecyltrichlorosilane (Sigma). Liquid PDMS (Sylgard 184, Dow Corning) was cured at 100 °C for 2 h after pouring over the master template. The top view of the fabricated PDMS stamp bearing 20 μm elevated lanes and 40 μm spacing among the lanes is shown in Figure S3, Supporting Information. For inking purposes, fabricated PDMS stamps were immersed with fibronectin dissolved in phosphate buffer saline (PBS) solution (PAA) (50 μg/mL) for 1 h followed by blow drying with pressurized purified nitrogen gas.

Micropatterning of hMSCs. The modified microcontact printing procedure from the method described by Li et al. was used[32] and illustrated in Figure 1a. Lab Tek two well chambered cover glasses were treated with freshly prepared piranha solution followed by inking with 3% (3-aminopropyl) triethoxysilane (APTES) (Sigma) for an hour. (*CAUTION*: "Piranha" solution reacts violently with organic materials; it must be handled with extreme care.) After that, cover glasses were washed with ultrapure water several times to remove any excess unbound APTES. Then 2.5% glutaraldehyde solution was added to treat APTES coated cover glasses for an hour followed by washing with ultrapure water. The PDMS stamp patterned surface was then covered with fibronectin dissolved in PBS solution (50 μg/mL) for 1 h and blown dry with pressurized purified nitrogen gas. Fibronectin inked stamps were placed in conformal contact with glutaraldehyde treated cover glasses for 1 h. The unpatterned region was then passivated with freshly prepared 2% bovine serum albumin (BSA) (Invitrogen) for 1 h at 37 °C to avoid nonspecific attachment of the cells on the nonprinted region. Glass substrates were washed several times with PBS to remove the excess bovine serum albumin prior to cell seeding. All glass substrates were UV sterilized for 15 min before cell seeding. Finally, hMSCs were seeded at a density of 2−3 × 10^3 cells cm^{-2}. After 20−30 min, unattached cells were washed with PBS followed by addition of fresh culture medium. Culture medium was changed after every 2−3 days.

Cell Culture. Human bone marrow derived cryopreserved hMSCs were obtained from Lonza (Cambrex) and cultured in low glucose Dulbecco's Modified Eagle's Medium (DMEM) containing L-glutamine (Sigma-Aldrich) supplemented with 10% FBS (PAA) and 1% antibiotic/antimycotic solution (PAA). Cultured hMSCs were incubated at 37 °C in a humidified atmosphere of 5% CO_2. 0.25% trypsin-EDTA (Invitrogen) was used for cell detachment purposes. hMSCs from passage 5 were used to perform experiments mentioned herein.

Immunostaining and Microscopy. The myocardial linage commitment of hMSCs was revealed by β-myosin heavy chain (β-MHC) immunostaining. Cells were fixed with 4% paraformaldehyde solution for 5−10 min followed by permeabilization with 0.1% Triton X-100 for 5 min. Cells were then blocked with 5% bovine serum albumin in PBS for 1 h before incubating with mouse monoclonal anti human cardiac myosin heavy chain primary antibodies (1:400, Abcam) overnight at 4 °C. Following which, the samples were washed with PBS and labeled with Alexa Fluor 488 goat anti mouse IgG (1:400, Molecular probes). Cell nuclei were counter stained with 4′-6-diamidino-2-phenylindole (DAPI) (1:400, Chemicon). For cell cytoskeleton staining, cells were stained with tetramethyl rhodamine iso-thiocyanate (TRITC) conjugated-phalloidin (1:400, Chemicon). Validation of cardiac myosin heavy chain antibodies performance was done by using differentiated C2C12 murine myoblasts as a positive control, and samples without primary antibodies served as negative control. Images were taken with the Eclipse 80i upright microscope (Nikon) using a 20× objective lens and analyzed with ImageJ 1.44f software. Later, in this section, total internal reflection fluorescence (TIRF) imaging of F-actin was explained in detail.

A sequential multiple immunostaining technique was employed to label the active ITG-β_1 population in hMSCs. Cells were fixed with paraformaldehyde solution and Triton X-100 solution as mentioned earlier. Freshly made 5% normal goat serum (NGS) was used as blocking agent. For active ITG-β_1 staining, samples were incubated
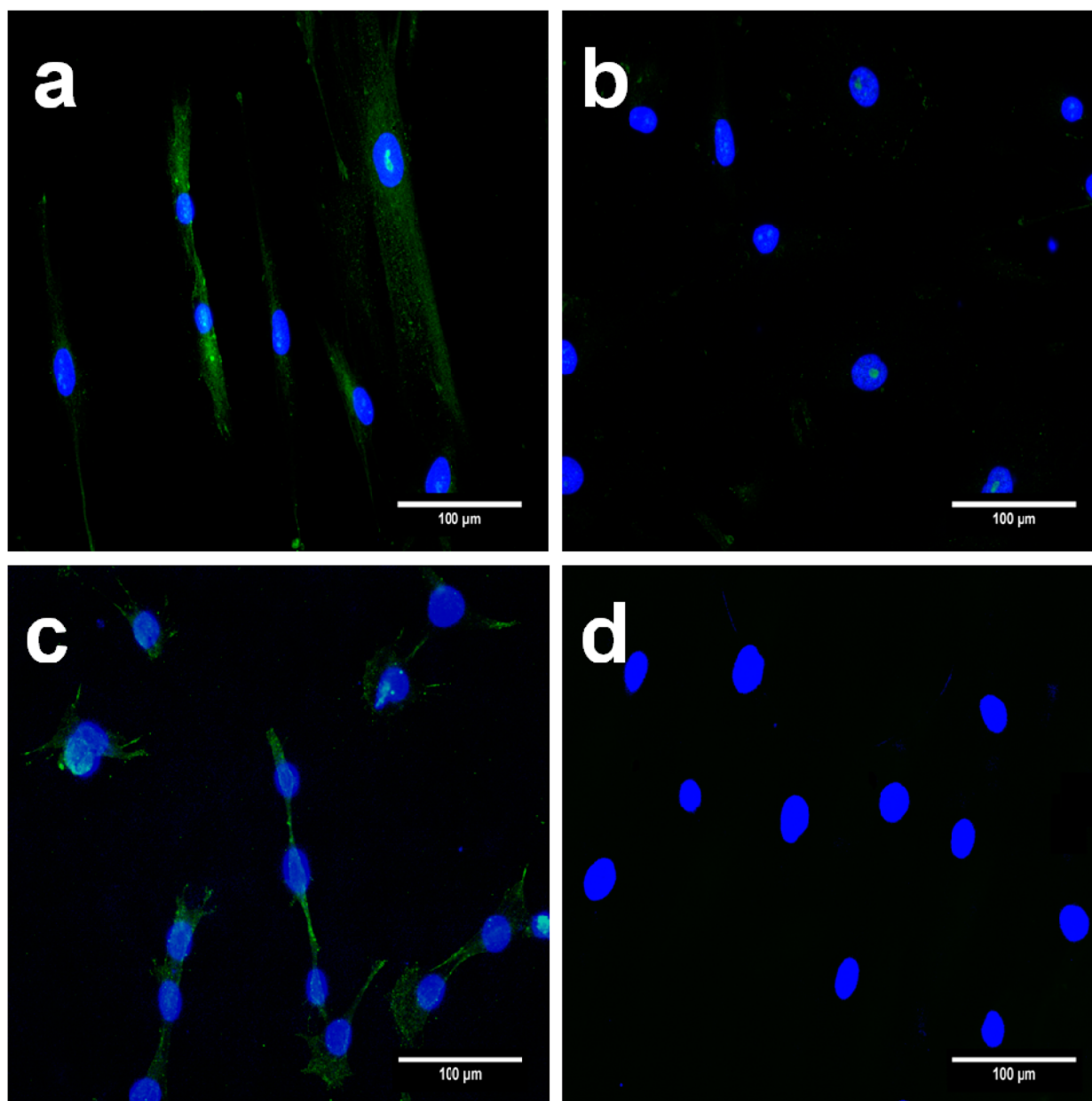
Figure 2. Immunodetection of cardiac marker (β-MHC) after 5 days of culture. Significant expression of β-MHC (green) was observed in the patterned group (a) but not for the unpatterned group (b). Specificity of primary antibodies was testified by using positive control. C2C12 murine myoblasts were induced to differentiate in the presence of 2% horse serum and stained for cardiac marker after 5 days of culture (c). Negative control in the absence of β-MHC primary antibodies was used to validate the specific binding of secondary antibodies (d). The scale bar is 100 μm.

with monoclonal mouse anti integrin β_1 IgG (1:200, Millipore) and counter stained with Alexa Fluor 647 goat anti mouse IgG (1:100, Invitrogen) followed by washing with PBS containing 0.5% v/v Tween-20. For β myosin heavy chain staining, samples were again treated with polyclonal rabbit anti MYH 7 IgG (1:200, Aviva Systems Biology) and incubated with Alexa Fluor 488 goat anti rabbit IgG (1:100, Invitrogen).

Imaging of β-MHC, ITG-β_1, and F-actin expressions was performed on a customized free space coupled TIRF system attached to an inverted Olympus IX-71 microscope capable of single molecule localization imaging. A 100×/1.49 TIRF Olympus objective lens was used for TIRF imaging. Lasers were merged using the suitable dichroics and acousto-optic tunable filter (AOTF) and reflected to the sample using a Semrock quadband filter. Appropriate emission filters were used for imaging individual molecules. A high sensitive liquid cooled Evolve 512 (Photometrics, USA) camera was used for detecting individual molecules. Further an intermediate zoom lens of

1.6× was used in the light path to generate wide field TIRF images with a resolution of 100 nm per pixel. Single molecule images were acquired using the Metamorph software, and the QuickPALM laser control software was used to control the acousto-optic tunable filter.

Prior to direct stochastic optical reconstruction microscopy (dSTORM) imaging, cells were embedded in buffer supplement with β-mercaptoethylamine (MEA, Sigma) with a final concentration of 100 mM at pH 8. Reconstructed images were obtained by direct iterative stochastic activation of subsets of Alexa Fluor 647 molecules and subsequent position determination by applying simultaneous excitation at 647 and 405 nm. LD 647 nm (150 mW) topitca laser and LD 405 nm (100 mW) cube coherent laser were used for fluorophore activation and dSTORM imaging purposes. Laser powers were selected in such a way that activated fluorophores (fluorescent ON state) were spaced further apart than their resolution limit to localize individual fluorophores.[27] Typically, 10 000−15 000 frames were recorded at a frame rate of 60 frames/second, resulting in acquisition
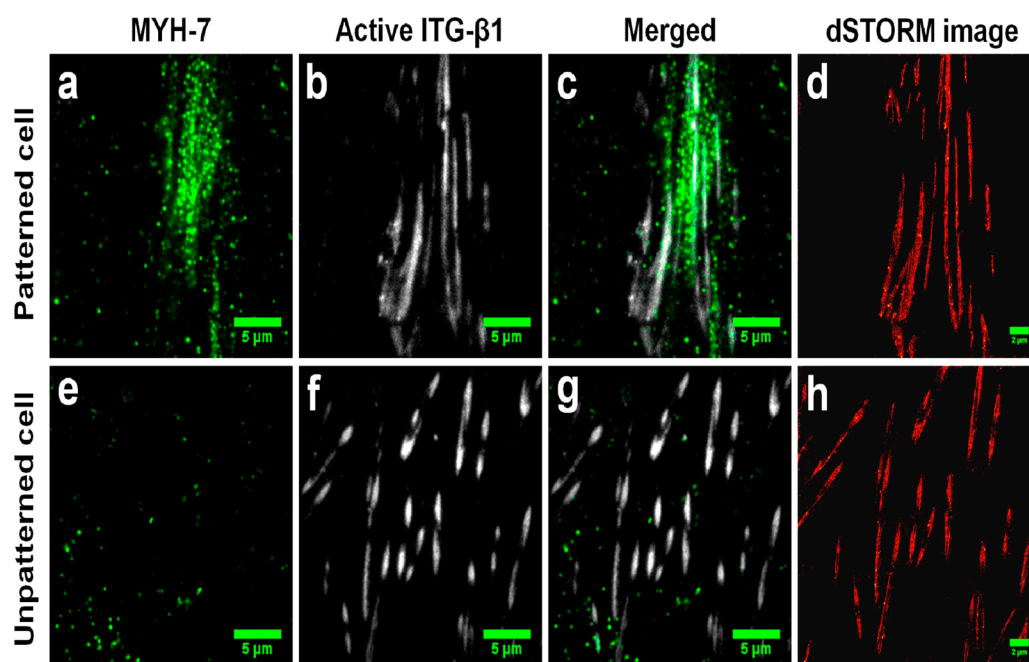
Figure 3. TIRF images of cells from both groups showing the positive (a) and negative (e) expression of cardiac marker (MYH-7). Active ITG-β_1 FAs distribution from respective location of cells was captured and demonstrated in panels (b, f). Merged images of MYH-7 expression and ITG-β_1 FAs distribution were presented in panels (c, g), while panels (d) and (h) indicated the reconstructed super-resolution images of ITG-β_1 FAs distribution. The scale bar is 5 μm in panels (a), (b), (c), (e), (f), and (g) and 2 μm in panels (d) and (h).

time of less than 5 min for a single data set. Super-resolution images were reconstructed using rapidSTORM with a final pixel size of 10 nm. The above mentioned conditions helped to keep fluorophore molecules in the fluorescent ON state for several frames after excitation and, in turn, detected thousands of photons per fluorophore.

Image Analysis and Statistical Study. A total of 20 cells were analyzed in each experimental group to perform the microscale distribution study. FA parameters like length and width were calculated by the "Measure" function of ImageJ software. Six cells were analyzed in each experimental group for nanoscale distribution study of integrin clusters. Individual integrin cluster area and total number of integrin clusters per FA were measured by using the same ImageJ software. Briefly, we marked the area of a focal adhesion and removed the remaining portion of the image. Then, the image was converted to an 8 bit image, and the "Adjust threshold" function was used to adjust the threshold of the image automatically. Finally, the "Analyze particles" function of ImageJ was used to analyze the individual integrin cluster area and to count the number of integrin clusters. Fluorescence intensity of integrin clusters was measured by the "plot profile" function of ImageJ. The one-way ANOVA method was used to perform the statistical analysis. A P-value <0.05 was considered statistically significant.

RESULTS AND DISCUSSION

Microcontact printing is a facile and versatile method to study the cell-material interactions.[8,33,34] Fibronectin micropatterning efficiency was validated with the immunostaining method (Figure S3, Supporting Information). hMSCs adhesion onto 20 μm wide fibronectin strips was observed within a few minutes after cell seeding and elongated cell morphology was confirmed with an optical microscope (Figure 1b).

MHC genes are one type of significant genes that play a vital role during the genetic program responsible for myogenesis.[35] β-MHC (isoform of MHC) is expressed predominantly in human ventricular myocardium and serves as a mature marker of cardiomyogenesis. Conversely, compromised β-MHC functionality in the form of mutations is responsible for various
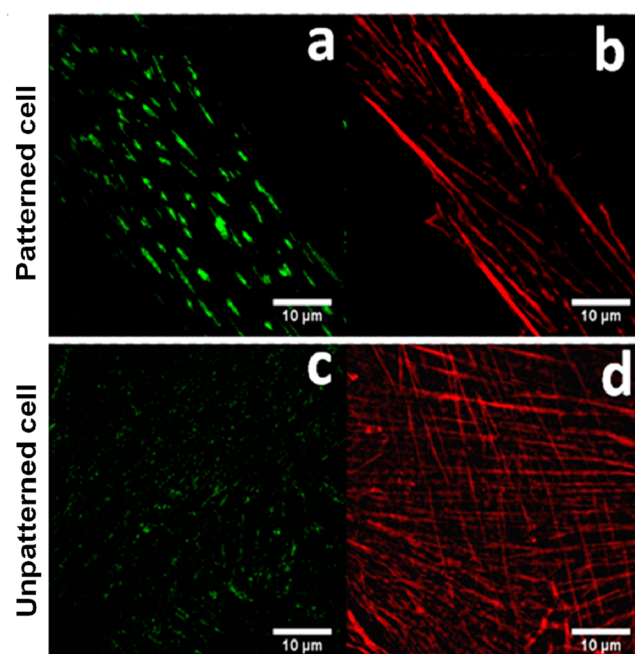

Figure 4. TIRF imaging was used to check the ITG-β_1 FAs expression and the alignment of cytoskeleton from both experimental groups. Patterned cells showed distinct recruitment of ITG-β_1 FAs (a) and well-aligned actin filaments morphology (b). In stark contrast, punctate and dotlike ITG-β_1 FAs (c) along with randomly distributed actin filaments network were observed in the unpatterned cell (d). The scale bar is 10 μm.

cardiomyopathy.[36] Therefore, β-MHC was selected as a reliable indicator of cardiomyogenic activity during experiments. Immunostaining of β-MHC revealed their restricted expression to the patterned cells adopting elongated morphology but not for randomly oriented unpatterned cells after 5 days of cell
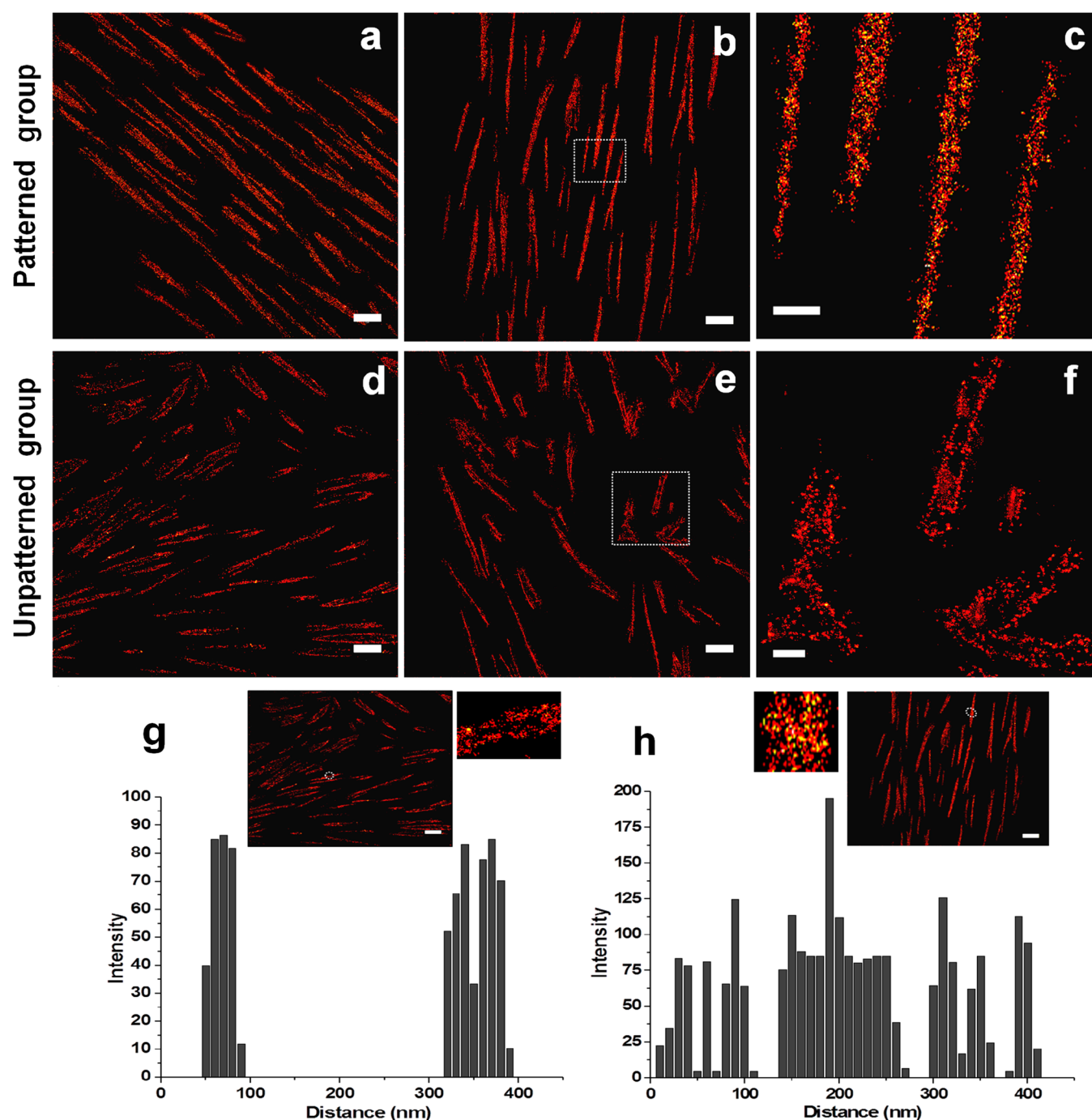
15690

dx.doi.org/10.1021/am504407n | *ACS Appl. Mater. Interfaces* 2014, 6, 15686−15696

Figure 5. Reconstructed super-resolution images of ITG-β_1 FAs from patterned (a–c) and unpatterned cells (d–f). Panels (c) and (f) displayed the magnified areas represented in panels (b) and (e), respectively. Histograms showing the integrin clusters distribution inside the marked FA area from the unpatterned cell (g) and the patterned cell (h). The scale bar is 2 μm in panels (a), (b), (d), and (e) and 500 nm in (c) and (f). The scale bar is 500 nm in panels g and h.

culture (Figure 2). This observation is in agreement with our previous findings, where hMSCs seeded over poly(lactic-*co*-glycolic acid) (PLGA) films with 20 μm wide patterned fibronectin strips showed a similar trend of elongated morphology with much smaller area of coverage.[23] Additionally, real-time polymerase chain reaction (PCR) data from similar previous findings showed that, after 5 days of culture, a distinct increase in various cardiomyogenic genes expression was observed with MyoD, MyF5, GATA4, NKX2-5, MHC, and cTnI displaying 4.2-, 3.9-, 3.7-, 3.0-, 3.3-, and 2.9-fold higher expression, respectively (compared to unpatterned hMSCs).

Further, to check the sustainability of lineage commitment of patterned hMSCs, hMSCs were cultured on a similar fibronectin patterned surface for a duration of 3 weeks and β-MHC immunostaining was performed. It was observed that patterned hMSCs sustained the myocardial lineage commitment even after 3 weeks (Figure S4, Supporting Information).

To investigate the active ITG-β_1 distribution in myocardial lineage committed hMSCs, we located the β-MHC positive cells with TIRF imaging followed by the inspection of their active ITG-β_1 population with a super-resolution imaging technique. A double immunostaining procedure was carried
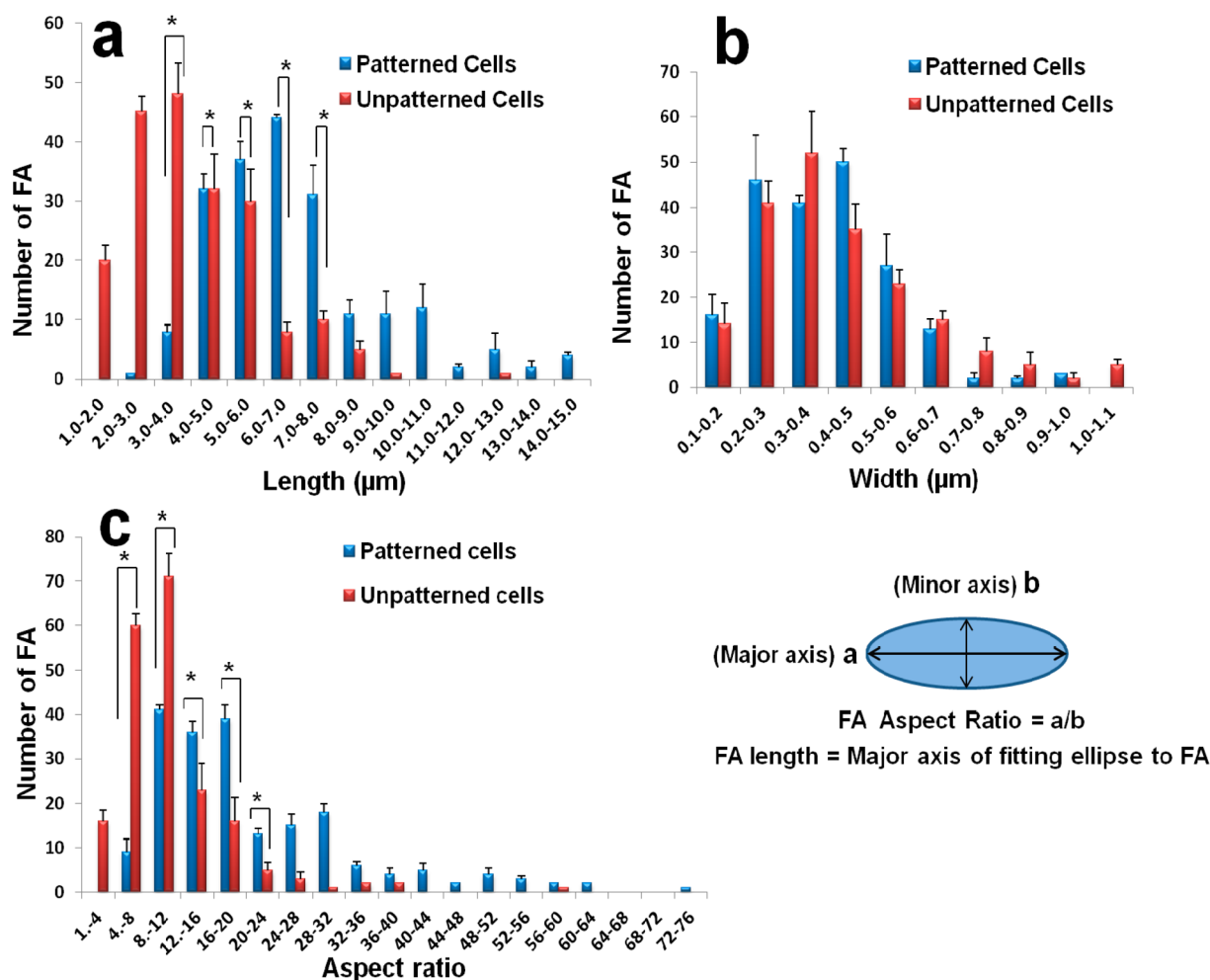
15691

dx.doi.org/10.1021/am504407n | *ACS Appl. Mater. Interfaces* 2014, 6, 15686–15696

Figure 6. ITG-β_1 FA morphological studies. Graphs (a−c) represent the length, width, and aspect ratio of FAs from patterned and unpatterned hMSCs after 5 days. Bars represent standard deviation among three samples of each experimental group ($n = 20$). *$p < 0.05$ between patterned and unpatterned groups.

after 5 days of culture (Figure S5, Supporting Information) to label β-MHC and ITG-β_1 of cells. Immunostaining was done by using the sequential approach,[37] which was more reliable in our system. The greatest advantage of sequential staining is that the cross-reactivity of antibodies can be minimized. TIRF images of myosin heavy chain (coded by MYH-7 gene) expression (Figure 3a) and ITG-β_1 FAs (Figure 3b) from same location in patterned cells were obtained. It was consistently observed that long and aligned active ITG-β_1 FAs were exclusively expressed in patterned cells. In contrast, unpatterned cells did not show any evident up-regulation of cardiomyogenic expression (Figure 3e) and, also, short and less aligned active ITG-β_1 FAs were sighted in an unpatterned cell (Figure 3f). Moreover, patterned cells not only recruited elongated active ITG-β_1 FAs but also formed a well-organized actin filaments network (Figure 4). On the other hand, punctate and dotlike active ITG-β_1 FAs along with a randomly distributed cytoskeleton were observed in the unpatterned cells. These results were consistent with a previous report where distinct recruitment of larger and elongated structures of ITG-β_3 were observed in hMSCs grown on micropatterned PDMS with stiffness of 12.6 kPa.[8] This study postulated that elongated FAs and aligned cytoskeleton contribute to up-regulated cardiomyogenic expression in patterned hMSCs. On the basis of the above observations, we conclude that the development of integrin FAs

in cells is directed by the geometry of the ECM pattern. Also, we hypothesize that the ECM patterned surface would direct a certain spatial integrin distribution pattern formation which is responsible for the mechanotransduction event of cell differentiation.

To investigate the spatial distribution of active ITG-β_1 at the receptor level, the super-resolution imaging technique was applied as it can resolve fluorescence images with lateral resolution down to 20 nm.[27,38] dSTORM images of active ITG-β_1 FAs from the same locations in hMSCs cultured on the ECM patterned surface or without the ECM patterned surface are shown in Figure 3d,h, respectively. Moreover, we used the dSTORM images (Figure 5) of ITG-β_1 FAs to further study the microscale distribution of ITG-β_1 FAs from both experimental groups. Variables such as FA length, FA width, FA aspect ratio (AR), and FA alignment were analyzed using ImageJ software. A higher AR value indicates more elongated ITG-β_1 FAs. AR can be calculated using the expression mentioned in Figure 6. A statistical study was performed on a total of 200 ITG-β_1 FAs from three samples of each experimental group. 10−12 ITG-β_1 FAs were selected from each cell, and 7−8 cells were selected per sample from each experiment group.

By day 5, long ITG-β_1 FAs were observed in hMSCs cultured on the ECM pattern surface (Figure 6a). Most of the FAs were 4−8 μm in length, and few FAs registered length up to 15 μm.
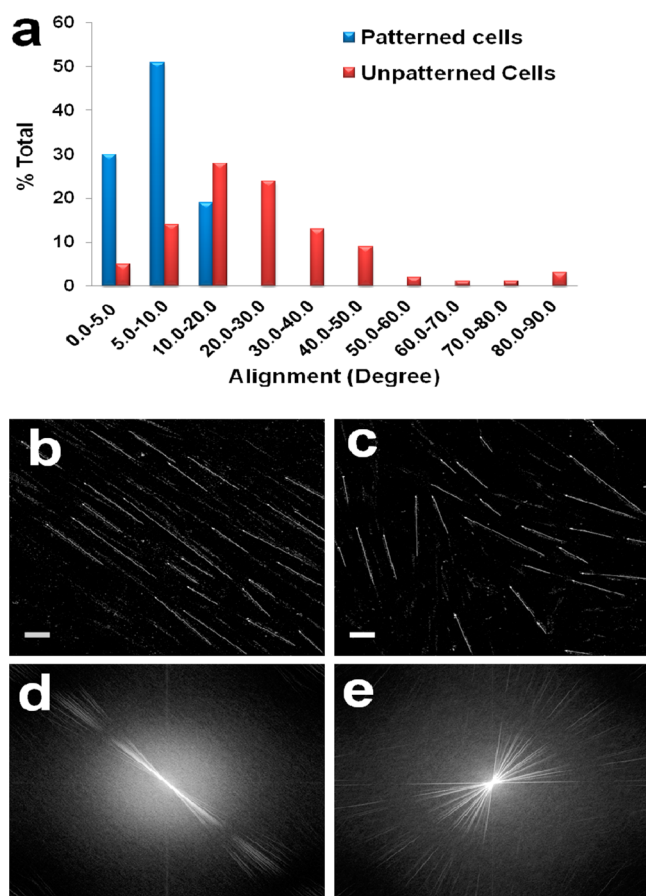
Figure 7. (a) Quantitative study of alignment of ITG-β_1 FAs from both experimental groups ($n = 5$). ITG-β_1 FAs from patterned and unpatterned groups were manually marked as shown in panels (b) and (c), respectively. (d) FFT analysis of the patterned cell (b) showed the definite alignment of FAs and (e) FFT analysis of the unpatterned cell (c) represented randomly oriented FAs. The scale bar is 2 μm in panels (b) and (c).

ITG-β_1 FAs expressed in unpatterned hMSCs differed strikingly with patterned cells in the case of the length parameter. Most cells from the unpatterned group showed short ITG-β_1 FAs with length ranging from 1 to 5 μm. In addition, ITG-β_1 FAs in patterned cells showed higher AR values, indicative of elongated morphology (Figure 6c). On the contrary, AR values for ITG-β_1 FAs in unpatterned cells implied less elongated morphology. There was no significant difference in the case of the ITG-β_1 FAs width for both experimental groups, mostly lying in the range of 200−500 nm (Figure 6b). A quantitative study of integrin FAs orientation was performed on day 5 of cell culture. Integrin FAs of unpatterned cells were randomly oriented with degrees of alignment from 0° to 90°, while integrin FAs of patterned cells were better aligned (Figure 7a). Alignment of integrin FAs along the micropattern axis was observed on day 5, with maximum angular distribution of around 5°−10°. Integrin FAs from both experimental groups were characterized by 2-D fast Fourier transform (FFT) analysis which converts spatial information into mathematically defined optical data. The 2-D FFT frequency plot reflects the degree of integrin FAs alignment by depicting the grayscale pixels distributed in patterns around the origin. The 2-D FFT images (Figure 7d,e) revealed that ITG-β_1 FAs in patterned cells were much more aligned than their unpatterned

counterparts. Also, angular distribution of ITG-β_1 FAs from both groups was determined by the circular analysis method which reconfirmed the results observed during FFT analysis (Figure S7, Supporting Information).

Altogether, the patterned group exhibited long, aligned, and elongated ITG-β_1 FAs in comparison to the unpatterned group. Cardiomyogenic differentiation in patterned cells might result from the activation of ITG-β_1 and other integrins that subsequently trigger the corresponding downstream signaling pathways. As reported by another group, 8−30 μm long supermature FAs consisting of integrins $\alpha_v\beta_3$ and $\alpha_5\beta_1$ along with particular anchorage proteins were observed in cultured myofibroblasts.[39] The formation of supermature FAs, which control the recruitment of α-smooth muscle actin (α-SMA) to preexisting stress fibers and the recruitment process, was driven by specific tension generated by a supermature FA itself.[40] It is a well-known fact that mechanical force applied to the focal adhesion is channeled to the cell nucleus via F-actin.[41] This force acting on the nucleus has the ability to alter the gene expression and DNA replication which in turn can determine cell fate. Previously, we reported that elongated FAs triggered the formation of aligned stress fiber and recruitment of myosin light chain kinase (MLCK), a regulator of cell contraction.[8] MLCK along with actomyosin-IIA complex can generate optimal cytoskeletal tension by reorganizing the stress fiber assembly to induce myocardial lineage commitment in patterned hMSCs. Consistent with these previous findings, this study also demonstrated the development of elongated active ITG-β_1 FAs in patterned cells which might be regulating the intracellular tension by affecting the development of cytoskeletal organization and subsequently driving cardiomyogenic differentiation of hMSCs.

Super-resolution imaging revealed that active ITG-β_1 FAs were composed of thousands of tiny active ITG-β_1 clusters (Figure 5). Hence, it is plausible to investigate the nanoscale distribution of active ITG-β_1 clusters inside the FAs from both experimental groups. Remarkably, in patterned cells, active ITG-β_1 clusters were distributed uniformly within FAs, whereas active ITG-β_1 clusters of unpatterned cells were expressed at the periphery of FAs. Integrin clusters distribution in a single FA of unpatterned cell was quantified (Figure 5g) with adjacent clusters being found to be spaced apart by more than 200 nm. Integrin clusters distribution from FA of patterned cells however demonstrated the equal distribution (Figure 5h). Previous findings showed that FAs were clustered at the edges of ECM patterns or ECM coated biophysical cues.[33,42,43] Researchers coined the term "edge effect" to describe this phenomenon and concluded that it was the outcome of equilibrium between the available potential adhesion sites and cellular traction forces.[44] Also, it was noticed that FAs interacting with these biophysical cues or patterns were frequently connected to each other by the network of actin bundles.[33,43,44] Actin bundle network helps to withstand traction forces and distribute the cellular tension exerted by the cell.[45] It has been demonstrated that integrins and anchorage proteins located directly at the edge of biophysical cues bear the highest mechanical tension.[44] We believe that forces applied on the substrate by unpatterned cells after 5 days could be higher than that of patterned cells, as evident by a higher spreading area. Therefore, to counter traction forces, unpatterned cells may further recruit more FAs with focal adhesion components at their periphery. This notion is in line with a previous study that demonstrated a concomitant increase
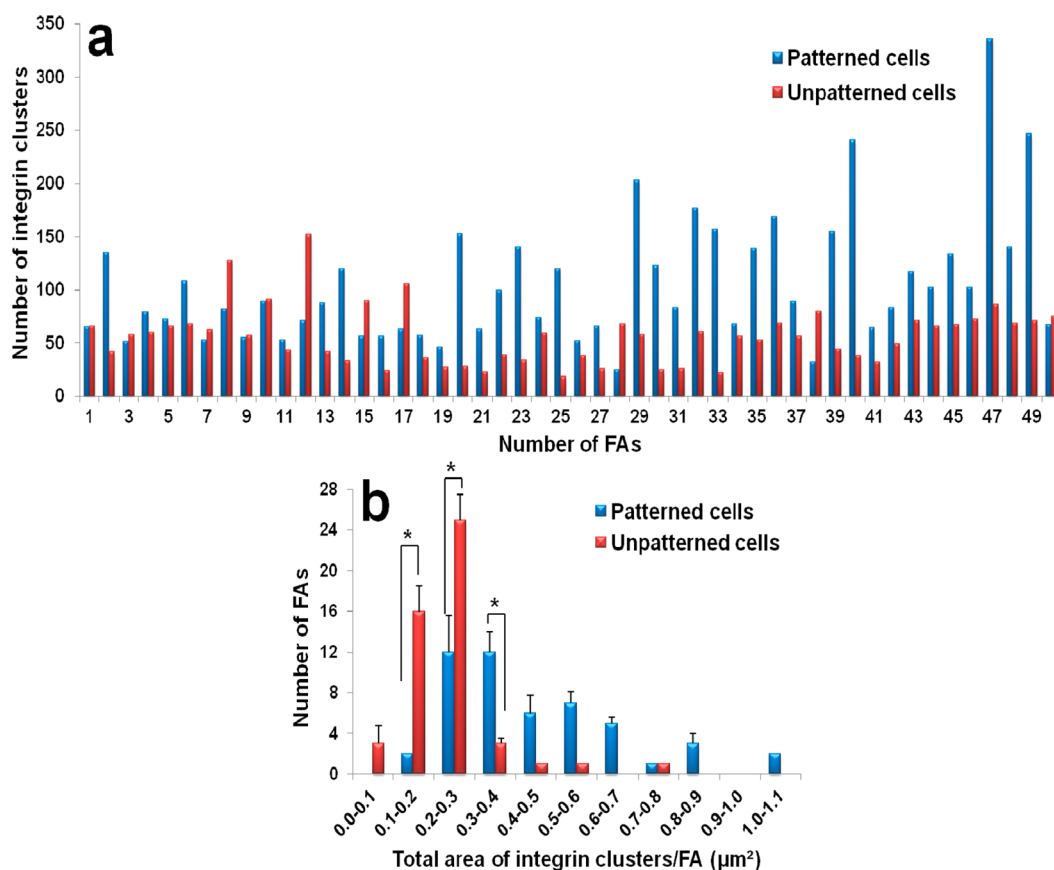
Figure 8. (a) Histogram showing the number of integrin clusters present in respective FA from patterned and unpatterned cell groups. (b) Quantitative analysis of total area of integrin clusters per FA from both experimental groups. Bars represent standard deviation among three samples of each experimental group ($n = 6$). *$p < 0.05$ between patterned and unpatterned groups.

in the recruitment of focal adhesion components (integrins and anchorage proteins) and traction force when the FAs are mechanically perturbed.[46] Therefore, we quantified the distribution of integrin clusters in FAs belonging to both experimental groups. A higher number of integrin clusters were consistently observed for most of the FAs in the patterned cells compared to the unpatterned group (Figure 8a). The total number of integrin clusters in patterned FAs was 5219 ± 461, whereas it decreased to 2830 ± 276 in unpatterned FAs. The estimated value of density of integrin clusters in patterned FA and unpatterned FA was found to be 27 ± 2 and 18 ± 4 clusters per μm^2, respectively. It was obvious that the total area occupied by integrin clusters per individual FA was larger for FAs from patterned cells (Figure 8b). Most of the patterned FAs displayed a total area of integrin clusters per FA in the range of $0.2-0.7$ μm^2, while the unpatterned FAs were lying in the range of $0.1-0.3$ μm^2. In short, the nanoscale distribution of active ITG-β_1 clusters differs widely in FAs from both groups.

CONCLUSION

In summary, we investigated the cell-material interactions at integrin receptor level during induction of cardiomyogenic differentiation in hMSCs using the TIRF system as well as super-resolution imaging. More importantly, we emphasized the role of active ITG-β_1 and its distribution during myocardial lineage commitment of hMSCs. It was revealed that distribution of active ITG-β_1 FAs was varied considerably in patterned and unpatterned cells. We confirmed that micro-

patterning was involved in inducing longer and elongated active ITG-β_1 FAs in patterned cells. In addition, it was established that these long and aligned FAs were involved in myocardial lineage commitment of patterned cells. We found that ITG-β_1 FAs in patterned cells were aligned to pattern direction. Most of them showed maximal angular distribution around $5°-10°$ relative to the pattern axis. The angular distribution study demonstrated that initial direction of integrins in early developmental stage of FAs plays an important role in cell orientation. Nanoscale distribution of active ITG-β_1 clusters within FAs was analyzed using super-resolution imaging. It was observed that, in patterned cells, ITG-β_1 clusters were distributed uniformly in FAs. On the other hand, in unpatterned cells, ITG-β_1 clusters were expressed at the periphery of FAs. The revelation of the distinct difference in the integrin clustering patterns of control and cardiomyogenic committed cells using advanced microscopic techniques that enable imaging of pivotal small-scale cellular components such as the integrins with submicron scale resolution could pave the way into deeper understanding of cell-material interaction and subsequent mechanotransduction of signals at the cell-material interface. From an engineering perspective, this interesting observation could provide invaluable scaffold design ideas for better control and manipulation of stem cell differentiation. At this stage, it is hypothesized that the integrin patterns would result in significantly different traction forces of the two experimental groups which in turn would trigger different signaling pathways. The next stage of work would delve deeper into the mechanotransduction route.

AUTHOR INFORMATION

Corresponding Author

*E-mail: lptan@ntu.edu.sg. Tel.: +65 67906186. Fax: +65 67909081.

REFERENCES

(1) Au, P.; Tam, J.; Fukumura, D.; Jain, R. K. Bone Marrow-Derived Mesenchymal Stem Cells Facilitate Engineering of Long-Lasting Functional Vasculature. *Blood* **2008**, *111*, 4551−4558.

(2) Tan, G.; Shim, W.; Gu, Y.; Qian, L.; Chung, Y. Y.; Lim, S. Y.; Yong, P.; Sim, E.; Wong, P. Differential Effect of Myocardial Matrix and Integrins on Cardiac Differentiation of Human Mesenchymal Stem Cells. *Differentiation* **2010**, *79*, 260−271.

(3) Guilak, F.; Cohen, D. M.; Estes, B. T.; Gimble, J. M.; Liedtke, W.; Chen, C. S. Control of Stem Cell Fate by Physical Interactions with the Extracellular Matrix. *Cell Stem Cell* **2009**, *5*, 17−26.

(4) Ohlstein, B.; Kai, T.; Decotto, E.; Spradling, A. The Stem Cell Niche: Theme and Variations. *Curr. Opin. Cell Biol.* **2004**, *16*, 693−699.

(5) Leong, W. S.; Wu, S. C.; Pal, M.; Tay, C. Y.; Yu, H.; Li, H.; Tan, L. P. Cyclic Tensile Loading Regulates Human Mesenchymal Stem Cell Differentiation into Neuron-Like Phenotype. *J. Tissue Eng. Regener. Med.* **2012**, *6*, s68−79.

(6) Metallo, C. M.; Mohr, J. C.; Detzel, C. J.; de Pablo, J. J.; Van Wie, B. J.; Palecek, S. P. Engineering the Stem Cell Microenvironment. *Biotechnol. Prog.* **2007**, *23*, 18−23.

(7) Tay, C. Y.; Yu, H.; Pal, M.; Leong, W. S.; Tan, N. S.; Ng, K. W.; Leong, D. T.; Tan, L. P. Micropatterned Matrix Directs Differentiation of Human Mesenchymal Stem Cells towards Myocardial Lineage. *Exp. Cell Res.* **2010**, *316*, 1159−1168.

(8) Yu, H.; Tay, C. Y.; Pal, M.; Leong, W. S.; Li, H.; Li, H.; Wen, F.; Leong, D. T.; Tan, L. P. A Bio-Inspired Platform to Modulate Myogenic Differentiation of Human Mesenchymal Stem Cells through Focal Adhesion Regulation. *Adv. Healthcare Mater.* **2013**, *2*, 442−449.

(9) Yu, T.; Chua, C. K.; Tay, C. Y.; Wen, F.; Yu, H.; Chan, J. K. Y.; Chong, M. S. K.; Leong, D. T.; Tan, L. P. A Generic Micropatterning Platform to Direct Human Mesenchymal Stem Cells from Different Origins Towards Myogenic Differentiation. *Macromol. Biosci.* **2013**, *13*, 799−807.

(10) van der Flier, A.; Sonnenberg, A. Function and Interactions of Integrins. *Cell Tissue Res.* **2001**, *305*, 285−298.

(11) Humphries, J. D.; Byron, A.; Humphries, M. J. Integrin Ligands at a Glance. *J. Cell Sci.* **2006**, *119*, 3901−3903.

(12) Hynes, R. O. Integrins: Bidirectional, Allosteric Signaling Machines. *Cell* **2002**, *110*, 673−687.

(13) Harburger, D. S.; Calderwood, D. A. Integrin Signalling at a Glance. *J. Cell Sci.* **2009**, *122*, 159−163.

(14) Giancotti, F. G.; Ruoslahti, E. Integrin Signaling. *Science* **1999**, *285*, 1028−1032.

(15) Tay, C. Y.; Koh, C. G.; Tan, N. S.; Leong, D. T.; Tan, L. P. Mechanoregulation of Stem Cell Fate via Micro-/Nano-Scale Manipulation for Regenerative Medicine. *Nanomedicine* **2013**, *8*, 623−638.

(16) Petit, V.; Thiery, J. P. Focal Adhesions: Structure and Dynamics. *Biol.Cell* **2000**, *92*, 477−494.

(17) Sheetz, M. P.; Felsenfeld, D. P.; Galbraith, C. G. Cell Migration: Regulation of Force on Extracellular Matrix-Integrin Complexes. *Trends Cell Biol.* **1998**, *8*, 51−54.

(18) Damsky, C. H.; Knudsen, K. A.; Bradley, D.; Buck, C. A.; Horwitz, A. F. Distribution of the Cell Substratum Attachment (CSAT) Antigen on Myogenic and Fibroblastic Cells in Culture. *J. Cell Biol.* **1985**, *100*, 1528−1539.

(19) Fassler, R.; Rohwedel, J.; Maltsev, V.; Bloch, W.; Lentini, S.; Guan, K.; Gullberg, D.; Hescheler, J.; Addicks, K.; Wobus, A. M. Differentiation and Integrity of Cardiac Muscle Cells Are Impaired in the Absence of Beta 1 Integrin. *J. Cell Sci.* **1996**, *109*, 2989−2999.

(20) Adams, J. C.; Watt, F. M. Changes in Keratinocyte Adhesion during Terminal Differentiation: Reduction in Fibronectin Binding Precedes Alpha 5 Beta 1 Integrin Loss from the Cell Surface. *Cell* **1990**, *63*, 425−435.

(21) Yim, E. K.; Darling, E. M.; Kulangara, K.; Guilak, F.; Leong, K. W. Nanotopography-Induced Changes in Focal Adhesions, Cytoskeletal Organization, and Mechanical Properties of Human Mesenchymal Stem Cells. *Biomaterials* **2010**, *31*, 1299−1306.

(22) Tay, C. Y.; Setyawati, M. I.; Xie, J.; Parak, W. J.; Leong, D. T. Back to Basics: Exploiting the Innate Physico-Chemical Characteristics of Nanomaterials for Biomedical Applications. *Adv. Funct. Mater.* **2014**, DOI: 10.1002/adfm.201401664.

(23) Tay, C. Y.; Pal, M.; Yu, H.; Leong, W. S.; Tan, N. S.; Ng, K. W.; Venkatraman, S.; Boey, F.; Leong, D. T.; Tan, L. P. Bio-Inspired Micropatterned Platform to Steer Stem Cell Differentiation. *Small* **2011**, *7*, 1416−1421.

(24) Hell, S. W. Far-Field Optical Nanoscopy. *Science* **2007**, *316*, 1153−1158.

(25) Kanchanawong, P.; Shtengel, G.; Pasapera, A. M.; Ramko, E. B.; Davidson, M. W.; Hess, H. F.; Waterman, C. M. Nanoscale Architecture of Integrin-Based Cell Adhesions. *Nature* **2010**, *468*, 580−584.

(26) Rossier, O.; Octeau, V.; Sibarita, J.-B.; Leduc, C.; Tessier, B.; Nair, D.; Gatterdam, V.; Destaing, O.; Albigès-Rizo, C.; Tampé, R.; Cognet, L.; Choquet, D.; Lounis, B.; Giannone, G. Integrins β_1 and β_3 Exhibit Distinct Dynamic Nanoscale Organizations inside Focal Adhesions. *Nat. Cell Biol.* **2012**, *14*, 1057−1067.

(27) van de Linde, S.; Loschberger, A.; Klein, T.; Heidbreder, M.; Wolter, S.; Heilemann, M.; Sauer, M. Direct Stochastic Optical Reconstruction Microscopy with Standard Fluorescent Probes. *Nat. Protoc.* **2011**, *6*, 991−1009.

(28) Li, H.; Wen, F.; Wong, Y. S.; Boey, F. Y. C.; Subbu, V. S.; Leong, D. T.; Ng, K. W.; Ng, G. K. L.; Tan, L. P. Direct Laser Machining-Induced Topographic Pattern Promotes Up-Regulation of Myogenic Markers in Human Mesenchymal Stem Cells. *Acta Biomater.* **2012**, *8*, 531−539.

(29) Yu, H.; Lui, Y. S.; Xiong, S.; Leong, W. S.; Wen, F.; Nurkahfianto, H.; Rana, S.; Leong, D. T.; Ng, K. W.; Tan, L. P. Insights into the Role of Focal Adhesion Modulation in Myogenic Differentiation of Human Mesenchymal Stem Cells. *Stem Cells Dev.* **2013**, *22*, 136−147.

(30) Hescheler, J.; Fleischmann, B. K. Regulation of Voltage-Dependent Ca^{2+} Channels in the Early Developing Heart: Role of β_1 Integrins. *Basic Res. Cardiol.* **2002**, *97*, I153−I158.

(31) Maitra, N.; Flink, I. L.; Bahl, J. J.; Morkin, E. Expression of Alpha and Beta Integrins during Terminal Differentiation of Cardiomyocytes. *Cardiovasc. Res.* **2000**, *47*, 715−725.

(32) Li, H.; Zhang, J.; Zhou, X.; Lu, G.; Yin, Z.; Li, G.; Wu, T.; Boey, F.; Venkatraman, S. S.; Zhang, H. Aminosilane Micropatterns on Hydroxyl-Terminated Substrates: Fabrication and Applications. *Langmuir* **2009**, *26*, 5603−5609.

(33) Chien, F. C.; Kuo, C. W.; Yang, Z. H.; Chueh, D. Y.; Chen, P. Exploring the Formation of Focal Adhesions on Patterned Surfaces Using Super-Resolution Imaging. *Small* **2011**, *7*, 2906−2913.

15695

dx.doi.org/10.1021/am504407n | *ACS Appl. Mater. Interfaces* 2014, 6, 15686−15696

(34) Wilbur, J. L.; Kumar, A.; Kim, E.; Whitesides, G. M. Microfabrication by Microcontact Printing of Self-Assembled Monolayers. *Adv. Mater.* **1994**, *6*, 600−604.

(35) Morkin, E. Regulation of Myosin Heavy Chain Genes in the Heart. *Circulation* **1993**, *87*, 1451−1460.

(36) Villard, E.; Duboscq-Bidot, L.; Charron, P.; Benaiche, A.; Conraads, V.; Sylvius, N.; Komajda, M. Mutation Screening in Dilated Cardiomyopathy: Prominent Role of the Beta Myosin Heavy Chain Gene. *Eur. Heart J.* **2005**, *26*, 794−803.

(37) Christensen, N. K.; Winther, L. Multi-Staining Immunohistochemistry. In *IHC Staining Methods*, 5th ed.; Kumar, G. L., Rudbeck, L., Eds.; Dako: Carpinteria, California, 2009; Chapter 15, pp 103−109.

(38) Heilemann, M.; van de Linde, S.; Schuttpelz, M.; Kasper, R.; Seefeldt, B.; Mukherjee, A.; Tinnefeld, P.; Sauer, M. Subdiffraction-Resolution Fluorescence Imaging with Conventional Fluorescent Probes. *Angew. Chem., Int. Ed.* **2008**, *47*, 6172−6176.

(39) Dugina, V.; Fontao, L.; Chaponnier, C.; Vasiliev, J.; Gabbiani, G. Focal Adhesion Features during Myofibroblastic Differentiation Are Controlled by Intracellular and Extracellular Factors. *J. Cell Sci.* **2001**, *114*, 3285−3296.

(40) Hinz, B.; Dugina, V.; Ballestrem, C.; Wehrle-Haller, B.; Chaponnier, C. Alpha-Smooth Muscle Actin Is Crucial for Focal Adhesion Maturation in Myofibroblasts. *Mol. Biol. Cell* **2003**, *14*, 2508−2519.

(41) Wang, N.; Tytell, J. D.; Ingber, D. E. Mechanotransduction at a Distance: Mechanically Coupling the Extracellular Matrix with the Nucleus. *Nat. Rev. Mol. Cell Biol.* **2009**, *10*, 75−82.

(42) Chen, C. S.; Mrksich, M.; Huang, S.; Whitesides, G. M.; Ingber, D. E. Geometric Control of Cell Life and Death. *Science* **1997**, *276*, 1425−1428.

(43) Brock, A.; Chang, E.; Ho, C.-C.; LeDuc, P.; Jiang, X.; Whitesides, G. M.; Ingber, D. E. Geometric Determinants of Directional Cell Motility Revealed Using Microcontact Printing. *Langmuir* **2003**, *19*, 1611−1617.

(44) Lehnert, D.; Wehrle-Haller, B.; David, C.; Weiland, U.; Ballestrem, C.; Imhof, B. A.; Bastmeyer, M. Cell Behaviour on Micropatterned Substrata: Limits of Extracellular Matrix Geometry for Spreading and Adhesion. *J. Cell Sci.* **2004**, *117*, 41−52.

(45) Arnold, M.; Schwieder, M.; Blummel, J.; Cavalcanti-Adam, E. A.; Lopez-Garcia, M.; Kessler, H.; Geiger, B.; Spatz, J. P. Cell Interactions with Hierarchically Structured Nano-Patterned Adhesive Surfaces. *Soft Matter* **2009**, *5*, 72−77.

(46) Sawada, Y.; Sheetz, M. P. Force Transduction by Triton Cytoskeletons. *J. Cell Biol.* **2002**, *156*, 609−615.